2-D Load Transfer Control Considering Obstacle Avoidance and Vibration Suppression

Junichi Nakajima and Yoshiyuki Noda
Department of Mechanical Systems Engineering, University of Yamanashi,4-3-11, Takeda, Kofu, Yamanashi, Japan

Keywords: Load Transfer Control, Trajectory Optimization, Vibration Suppression, Obstacle Avoidance, Overhead Traveling Crane.

Abstract: This paper is concerned with an advanced transfer control for load transfer machines such as a crane. In the load transfer machine, it is required to carry the load efficiently and safety. In order to satisfy this requirement, fast transfer of load, obstacle avoidance and vibration suppression have to be accomplished in the load transfer system. Therefore in this study, the load transfer control system which the transfer trajectory on a plane is optimized in consideration of the vibration suppression, obstacles avoidance and fast transfer is proposed. Moreover, in order to optimize the trajectory in a short time, the fast solution approach is also proposed in this study. The effectiveness of the proposed transfer control system is verified by the experiments using the laboratory type overhead traveling crane system.

1 INTRODUCTION

In manufacturing and construction industries, a load transfer machine such as an overhead traveling crane and a gantry loader is used to carry a heavy load and to support the assembly of components. These transfer machines are required to reach at the target position in a short time and to avoid the obstacles on a plane(Kawakami, et al., 2003), (Negishi, et al., 2013). Furthermore, it is required to suppress the vibration of the transfer object in the overhead traveling crane and the gantry loader, because the next task after arriving at the target position is delayed by the vibration occurred. Therefore, there is a great hope that the load transfer machine has the control functions of the obstacles avoidance, the vibration suppression and fast transfer(Yano, et al., 2002).

In order to fulfill the above requirements, the transfer control systems have been proposed in the previous studies. Especially, a lot of transfer control systems for an overhead traveling crane have been proposed. The vibration suppression control to the load of the overhead crane using optimal control theory was proposed(Al-Garni, et al., 1995). The gain-scheduled control was applied for suppressing the vibration of the load with rope length varying(Takagi and Nishimura, 1998), (Harald and Dominik, 2009). The acceleration of the cart was shaped for eliminating the natural frequency element of the vibration(Murakami and Ikeda, 2006). However, these control systems are only for the swaying suppression of the load. In the 2-D load transfer system such as the overhead traveling crane without the vertical transfer, a path planning with obstacles avoidance is needed.

In studies of the path planning for transfer system, the path of the transfer object was derived by the potential method(Branner,et al., 2012), the probabilistic road map method(Yu-Cheng, et al., 2012), and predicting the action of the moving obstacle(Tamura, et al., 2013). In the study(Suzuki and Terashima, 2000), the potential method is used for deriving the path with obstacle avoidance, and the path is reshaped for suppressing the vibration. Since the reshaped path differs from the path for avoidance of obstacle derived from the potential method, the transfer object is in danger of collision with obstacle.

Therefore in this study, the 2-D load transfer control using the trajectory planning approach considering the obstacles avoidance, the vibration suppression and the fast transfer is proposed for the load transfer machine on a plane. In this approach, the trajectory of the cart can be derived by the optimization problem which minimizes the integral square error of the cart position and the target position, and energy of desired frequency bands. The natural frequencies of the vibration are assigned to the frequency bands in the cost function for vibration suppression. The optimization problem has the constraints on the acceleration, the

Nakajima J. and Noda Y..
2-D Load Transfer Control Considering Obstacle Avoidance and Vibration Suppression.
DOI: 10.5220/0005030806530660
In *Proceedings of the 11th International Conference on Informatics in Control, Automation and Robotics* (ICINCO-2014), pages 653-660
ISBN: 978-989-758-040-6

velocity, and the position of the cart. The obstacles are given as the constraints of the cart position. Moreover, in order to derive the trajectory in a short time, the fast solution of the trajectory planning is also proposed in this study. The effectiveness of the proposed transfer control system is verified by the experiments using the laboratory overhead traveling crane system.

2 REPRESENTATION OF LOAD TRANSFER SYSTEM

The load transfer system in this study consists of two position feedback control systems to the 2-D transfer machine with an input and state constraints as shown in Figure 1. These position feedback control systems are assigned orthogonally in the 2-D load transfer machine. $P(s)$ is shown as the transfer machine with vibration elements, $K(s)$ is shown as the feedback controller, and r, z_u and z_x are shown as the target position, the control input and the controlled variables, respectively. The observed variable y is the cart position which measured by the sensor such as a rotary encorder.

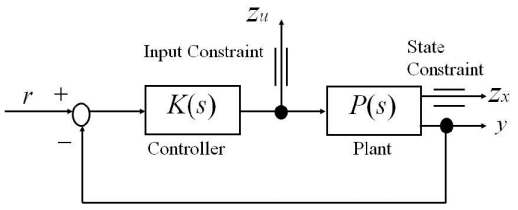

Figure 1: Position feedback control system in load transfer system

The model to transfer on X-axis in the orthogonal arrangement is described by the discrete time system as

$$x_x(k+1) = A_{clx}x_x(k) + B_{clx}r_x(k), \quad (1)$$
$$z_x(k) = C_{zclx}x_x(k) + D_{zxlx}r_x(k), \quad (2)$$
$$y_x(k) = C_{yclx}x_x(k) + D_{yclx}r_x(k). \quad (3)$$

Similarly, that on Y-axis is described as

$$x_y(k+1) = A_{cly}x_y(k) + B_{cly}r_y(k), \quad (4)$$
$$z_y(k) = C_{zcly}x_y(k) + D_{zxly}r_y(k), \quad (5)$$
$$y_y(k) = C_{ycly}x_y(k) + D_{ycly}r_y(k). \quad (6)$$

where $x_x(k) \subset R^n$ and $x\_y(k) \subset R^n$ are shown as the state vectors of each feedback system, and $z_x(k)$ and $z_y(k)$ are shown as the control variables with the constraints on each axis. The equation (1) is the state equation to transfer on X-axis. The equation (2) is output equation about controlled variable, and the equation (3) is the observation equation. The transfer on Y-axis is described similarly. The initial condition is as $x(0) = 0$ becouse of the transfer from a stationary state, and $z_x(k)$ and $z_y(k)$ has to be filled restrictions as

$$z_x(k) \in Z_x = \{z \mid\mid z_x \mid \leq z_{xc}\}, \forall k, \quad (7)$$
$$z_y(k) \in Z_y = \{z \mid\mid z_y \mid \leq z_{yc}\}, \forall k, \quad (8)$$

where z_{xc} and z_{yc} are the boundary parameters of the constraints.

3 TRAJECTORY PLANNING APPROACH

We propose the trajectory planning method with the time-series information by the optimization problem which is considered reaching a target position in a short time, suppressing the vibration, filling the constraints of the transfer machine, and obstacles avoidance for the load transfer system.

3.1 Cost Function

One of the purpose in this study is to minimize the cost function with the integral square error of the cart position y and the target position r_0 in order to transfer the target position in a short time, and the energy of the frequency bands to the varying natural frequency of the vibration in order to suppress the vibration which the naturel frequency is changed. The cost function is shown as

$$\begin{aligned} J = & w_1 \sum_{k=0}^{N-1} \mid r_{0x}(k) - y_x(k) \mid^2 \\ & + w_1 \sum_{k=0}^{N-1} \mid r_{0y}(k) - y_y(k) \mid^2 \\ & + w_2 \int_{v_1}^{v_2} \mid z_{ux}(v) \mid^2 dv + w_3 \int_{v_1}^{v_2} \mid z_{uy}(v) \mid^2 dv. \end{aligned} \quad (9)$$

In this cost function, r_{0x} and r_{0y} are the target position on X- and Y-axes, respectively. The first term in right side has the integral square error of the cart position y and the target position r_0, additionally the second term and the third term are the integral energy of the frequency bands (v_1 to v_2) on the control input on X- and Y-axes, respectively. And, $w_1 \geq 0$, $w_2 \geq 0$ and $w_3 \geq 0$ are the weight coefficients of scalar. Here, the control input and the controlled and observation

valuables can be derived from the equations (2) and (3) as

$$z_x(k) = \sum_{i=0}^{k-1} C_{zclx} A_{clx}^{k-i-1} B_{clx} r_x(i) + D_{zclx} r_x(k), \quad (10)$$

$$y_x(k) = \sum_{i=0}^{k-1} C_{yclx} A_{clx}^{k-i-1} B_{clx} r_x(i) + D_{yclx} r_x(k). \quad (11)$$

Here, the vectors of the input and the controlled variable are defined respectively as

$$Z_u = [z_u(0)\ z_u(1)\ \cdots\ z_u(n-1)]^T,$$
$$Z_x = [z_x(0)\ z_x(1)\ \cdots\ z_x(n-1)]^T. \quad (12)$$

Moreover, $R_x C R_{0x}$ and Y_x are the vectors consists of the elements $r_x(k) C r_{0x}(k)$ and $y_x(k)$, (k =0,1,$\cdots$,n-1). Therefore, the equations (10) and (11) can be represented as

$$Z_x = M_{zx} R_x\ ,\ Y_x = M_{yx} R_x, \quad (13)$$

where M_{zx} and M_{yx} are shown as

$$M_{zx} = \begin{pmatrix} D_{zclx} & 0 & \cdots & 0 \\ C_{zclx}B_{clx} & D_{zclx} & \cdots & \vdots \\ \vdots & \vdots & \ddots & 0 \\ C_{yclx}A_{clx}^{n-2} & \cdots & C_{zclx}B_{clx} & D_{zclx} \end{pmatrix}, \quad (14)$$

$$M_{yx} = \begin{pmatrix} D_{yclx} & 0 & \cdots & 0 \\ C_{yclx}B_{clx} & D_{yclx} & \cdots & \vdots \\ \vdots & \vdots & \ddots & 0 \\ C_{yclx}A_{clx}^{n-2} & \cdots & C_{yclx}B_{clx} & D_{yclx} \end{pmatrix}. \quad (15)$$

Moreover, M_{zy} and M_{yy} on Y-axis can be derived by similar process to the derivation on X-axis. Therefore, the first term without the weight coefficient of the cost function as shown in the equation (9) can be represented as

$$\begin{aligned} J_1 &= R_{0x}^T R_{0x} - R_x^T M_{yx}^T R_{0x} - R_{0x}^T M_{yx} R_x \\ &+ R_x^T M_{yx}^T M_{yx} R_x + R_{0y}^T R_{0y} - R_y^T M_{yy}^T R_{0y} \\ &- R_{0y}^T M_{yy} R_y + R_y^T M_{yy}^T M_{yy} R_y. \end{aligned} \quad (16)$$

In the equation (16), $R_{0x}^T R_{0x}$ and $R_{0y}^T R_{0y}$ are constant. Therefore, they are omitted from the cost function. And, $R_i^T M_{yi}^T R_{0i} (i = x, y)$ and these transposes are same value because of scalar. Therefore, the equation (16) can be organized as

$$\begin{aligned} \overline{J}_1 &= (R_x^T M_{yx}^T M_{yx} R_x - 2 R_x^T M_{yx}^T R_{0x}) \\ &+ (R_y^T M_{yy}^T M_{yy} R_y - 2 R_y^T M_{yy}^T R_{0y}). \end{aligned} \quad (17)$$

The second term in right side without the weight coefficient w_2 in the cost function as shown in the equation (9) can be represented by using discrete Fourier transform as

$$\begin{aligned} J_2 &= \int_{v_1}^{v_2} |\ z_{ux}(v)\ |^2\ dv = \int_{v_1}^{v_2} |\sum_{k=0}^{N-1} z_{ux}(k) e^{-jv\Delta Tk}|^2 dv \\ &= \int_{v_1}^{v_2} \sum_{k=0}^{N-1} z_{ux}(k) e^{-jv\Delta Tk} * \sum_{k=0}^{N-1} e^{jv\Delta Tk} z_{ux}(k) dv, \end{aligned} \quad (18)$$

where ΔT is a sampling period. By using the equation (12), the cost function J_2 can be represented as

$$J_2 = \int_{v_1}^{v_2} Z_{ux}^T E E^* Z_{ux} dv, \quad (19)$$

where E is as

$$E = [1 \quad e^{-jv\Delta T} \cdots e^{-jv\Delta T(n-1)}]^T. \quad (20)$$

E^* is the conjugate transpose matrix of E. Then, the equation (19) can be represented as

$$J_2 = Z_{ux}^T \int_{v_1}^{v_2} E E^* dv Z_{ux} = Z_{ux}^T M_e Z_{ux}, \quad (21)$$

where M_e is as

$$M_e = \int_{v_1}^{v_2} E E^* dv$$

$$= \begin{pmatrix} v_2 - v_1 & \frac{e^{jv_2\Delta T} - e^{jv_1\Delta T}}{j\Delta T} & \cdots & \frac{e^{jv_2\Delta T(n-1)} - e^{2jv_1\Delta T(n-1)}}{j\Delta T} \\ -\frac{e^{jv_2\Delta T} - e^{jv_1\Delta T}}{j\Delta T} & v_2 - v_1 & \ddots & \vdots \\ \vdots & \ddots & \ddots & \frac{e^{jv_2\Delta T} - e^{jv_1\Delta T}}{j\Delta T} \\ -\frac{e^{jv_2\Delta T(n-1)} - e^{2jv_1\Delta T(n-1)}}{j\Delta T} & \cdots & -\frac{e^{jv_2\Delta T} - e^{jv_1\Delta T}}{j\Delta T} & v_2 - v_1 \end{pmatrix}. \quad (22)$$

M_e in the equation (21) can be replaced to the symmetric matrix $\overline{M}_e$ shown as

$$J_2 = Z_{ux}^T M_e Z_{ux} = Z_{ux}^T (\frac{M_e + M_e^T}{2}) Z_{ux} = Z_{ux}^T \overline{M}_e Z_{ux} \quad (23)$$

where $\overline{M}_e$ is shown as

$$\overline{M}_e = \begin{pmatrix} v_2 - v_1 & \frac{\sin v_2\Delta T - \sin v_1\Delta T}{\Delta T} & \cdots & \frac{\sin v_2\Delta T(n-1) - \sin v_1\Delta T(n-1)}{\Delta T(n-1)} \\ \frac{\sin v_2\Delta T - \sin v_1\Delta T}{\Delta T} & v_2 - v_1 & \ddots & \vdots \\ \vdots & \ddots & \ddots & \frac{\sin v_2\Delta T - \sin v_1\Delta T}{\Delta T} \\ \frac{\sin v_2\Delta T(n-1) - \sin v_1\Delta T(n-1)}{\Delta T(n-1)} & \cdots & \frac{\sin v_2\Delta T - \sin v_1\Delta T}{\Delta T} & v_2 - v_1 \end{pmatrix}. \quad (24)$$

Z_{ux} can be represented as $Z_{ux} = M_{zux}R_x$ from the equation (13). Therefore, the second term J_2 in the cost function as shown in the equation (9) can be represented as

$$J_2 = R_x^T M_{zux}^T \overline{M}_e M_{zux} R_x. \quad (25)$$

Going through the same procedure as J_2, the third term J_3 in the equation (9), which is the integral energy on the frequency bands (v_1 to v_2) in Y-axis, can be derived as

$$J_3 = R_y^T M_{zuy}^T \overline{M}_e M_{zuy} R_y. \quad (26)$$

Summarizing the equations (17), (25) and (26), the cost function in the equation (9) can be represented as

$$\begin{aligned}\min_{R_x,R_y} J &= \min_{R_x,R_y}(w_1\bar{J}_1 + w_2 J_2 + w_3 J_3)\\ &= \min_{R_x,R_y}\{-2w_1(R_x^T M_{yx}^T R_{0x} + R_y^T M_{yy}^T R_{0y})\\ &\quad + R_x^T(w_1 M_{yx}^T M_{yx} + w_2 M_{zux}^T \overline{M}_e M_{zux})R_x\\ &\quad + R_y^T(w_1 M_{yy}^T M_{yy} + w_3 M_{zuy}^T \overline{M}_e M_{zuy})R_y\}. \quad (27)\end{aligned}$$

This cost function has the dynamics of the transfer system as represented in equation (13).

3.2 Input and State Constraints on Transfer System

From the equations (7) and (8), the input and state constraints of the 2-D load transfer machine can be represented as

$$|M_{zxx}R_x| \le Z_{xxc}\ , |M_{zux}R_x| \le Z_{uxc}, \quad (28)$$

$$|M_{zxy}R_y| \le Z_{xyc}\ , |M_{zuy}R_y| \le Z_{uyc}, \quad (29)$$

where Z_{xxc}, Z_{xyc}, Z_{uxc} and Z_{uyc} are the input and state constraints as

$$\begin{aligned}Z_{xxc} &= [z_{xc}\ \cdots\ z_{xc}]^T\ ,\ Z_{xyc} = [z_{yc}\ \cdots\ z_{yc}]^T\ ,\\ Z_{xuc} &= [z_{uxc}\ \cdots\ z_{uxc}]^T\ ,\ Z_{uyc} = [z_{uyc}\ \cdots\ z_{uyc}]^T. \quad (30)\end{aligned}$$

The trajectory planning in this study is performed on the finite time interval. In order to reach the transfer object to the target position (r_{0x}, r_{0y}) with stationary at the final time, the following equality constraints are given.

$$M_{fx}R_x = Z_{fx}\ ,\ M_{fy}R_y = Z_{fy}, \quad (31)$$

where M_{fx}, M_{fy}, Z_{fx} and Z_{fy} are as

$$M_{fx} = \begin{pmatrix} C_{yclx}A_{clx}^{N-2}B_{clx}\cdots C_{yclx}B_{clx} & D_{yclx} \\ C_{zclx}A_{clx}^{N-2}B_{clx}\cdots C_{zclx}B_{clx} & D_{zclx} \end{pmatrix}, \quad (32)$$

$$M_{fy} = \begin{pmatrix} C_{yclx}A_{cly}^{N-2}B_{cly}\cdots C_{yclx}B_{cly} & D_{yclx} \\ C_{zclx}A_{cly}^{N-2}B_{cly}\cdots C_{zclx}B_{cly} & D_{zclx} \end{pmatrix}, \quad (33)$$

$$Z_{fx} = \begin{pmatrix} r_{0x} \\ 0 \end{pmatrix}, \quad (34)$$

$$Z_{fy} = \begin{pmatrix} r_{0y} \\ 0 \end{pmatrix}. \quad (35)$$

The first, second and third rows in the equation (31) are for the terminate constraints of the cart position, velocity and acceleration, respectively. The reference trajectory optimization using the equations (27), (28), (29) and (31) is performed by a quadratic programming. However, since the reference trajectories on X- and Y-axes are designed independently, it does not include the function of the obstacle avoidance. In next section, we introduce the function of the obstacle avoidance.

3.3 Obstacle Represented by Constraint Condition

If we try to apply for the load transfer system such as an overhead traveling crane with some obstacles in the transfer space, we should design 2-D transfer trajectory which avoids the obstacles and does not excite the vibration. Therefore in this study, the obstacle area are defined as inequality constraints in the quadratic form, and they are given into the optimization problem shown in the previous section for planning the trajectory with the obstacles avoidance.

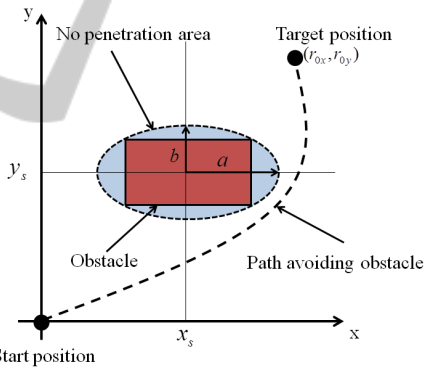

Figure 2: Path planning with obstacle avoidance.

In this approach, the obstacle is covered in the ellipse as shown in Figure 2. The inside of the ellipse is the no penetration area for planning the trajectory. Therefore, the following inequality constraint is given.

$$\frac{(y_x(k)-x_s)^2}{a^2} + \frac{(y_y(k)-y_s)^2}{b^2} - 1 \ge 0, \quad (36)$$

where (x_s,y_s) is shown as the center position of the ellipse, and a and b are shown as the length of the X- and Y-directions on the ellipse. For matrix representation of the equation (36), the following inequality equation is defined.

$$
\begin{aligned}
&(e_1M_{yx}R_x - e_1X_0)^T(e_1M_{yx}R_x - e_1X_0)/(a^2)\\
&+(e_1M_{yy}R_y - e_1Y_0)^T(e_1M_{yy}R_y - e_1Y_0)/(b^2) - 1\\
&= (R_x^T M_{yx}^T e_1^T e_1 M_{yx}R_x - 2X_0^T e_1^T e_1 M_{yx}R_x\\
&+X_0^T e_1^T e_1 X_0)/(a^2) + (R_y^T M_{yy}^T e_1^T e_1 M_{yy}R_y\\
&-2Y_0^T e_1^T e_1 M_{yy}R_y + Y_0^T e_1^T e_1 Y_0)/(b^2) - 1 \geq 0, \quad (37)
\end{aligned}
$$

where $e_1 = [1,0,0,0,\cdots,0] \in R^{1\times n}$, $X_0 = [x_0,x_0,\cdots,x_0]^T \in R^{1\times n}$, $Y_0 = [y_0,y_0,\cdots,y_0]^T \in R^{1\times n}$. The equation (37) shows the inequality equation at $k = 1$. At $k = 2$, $e_2 = [0,1,0,0,\cdots,0] \in R^{1\times n}$ is applied as the equation (37). Therefore, $e_i = [0,\cdots,0,1,0,\cdots,0] \in R^{1\times n}$ is defined for applying all of trajectory. The inequality constraint for obstacle avoidance is represented as

$$
\begin{aligned}
&(R_x^T M_{yx}^T \eta M_{yx}R_x - 2X_0\eta M_{yx}R_x\\
&+X_0\eta X_0)/(a^2) + (R_y^T M_{yy}^T \eta M_{yy}R_y\\
&-2Y_0\eta M_{yy}R_y + Y_0\eta Y_0)/(b^2) - \tilde{\eta} \geq 0, \quad (38)
\end{aligned}
$$

where,

$$\eta = [e_1^T e_1 \cdots e_k^T e_k \cdots e_n^T e_n]^T, \quad (39)$$

$$\tilde{\eta} = [e_1 e_1^T \cdots e_k e_k^T \cdots e_n e_n^T]^T. \quad (40)$$

Organizing the equation (38) into a quadratic form, the following equation can be derived.

$$
\begin{aligned}
&R_x^T(\frac{1}{a^2}M_{yx}^T\eta M_{yx})R_x + R_y^T(\frac{1}{b^2}M_{yy}^T\eta M_{yy})R_y\\
&-(\frac{2}{a^2}X_0\eta M_{yx})R_x - (\frac{2}{b^2}Y_0\eta M_{yy})R_y\\
&\geq -\frac{1}{a^2}X_0\eta X_0 - \frac{1}{b^2}Y_0\eta Y_0 + \tilde{\eta} \quad (41)
\end{aligned}
$$

By adding the equation (41) into the trajectory optimization in the previous section, the 2-D trajectory with function of the obstacles avoidance can be derived.

Therefore, the trajectory planning problem of the 2-D load transfer machine that is concerned with fast transfer control with vibration suppression and obstacles avoidance to a transfer object is resulted a quadratic programing problem with quadratic constraints. This quadratic programming problem can be solved by a sequential quadratic programming method.

4 FAST SOLUTION OF TRAJECTORY PLANNING

In this trajectory planning method proposed in this study, the calculation takes immense amount of time, because the trajectory represented by the sample number n should be solved by the quadratic programming problem with the quadratic constraints. In order to solve the problem in a short time, we propose the fast solution of the trajectory planning.

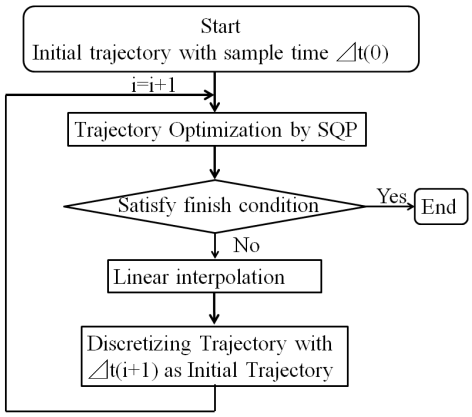

Figure 3: Iteration for fast solution of transfer trajectory.

The calculation time for planning the trajectory is decreased with decreasing the sample number n. Therefore, the fast solution method as shown in Figure 3 is proposed. In this method, the trajectory with the long sampling period is derived by the trajectory planning proposed in the previous section. Then, the discrete trajectory with the long sampling period is linearly-interpolated, and the interpolated trajectory is discretized with the shorter sampling period than that of the previous optimized trajectory. The trajectory optimization is performed with the discretized trajectory as the initial trajectory. By iterating the procedure as shown in Figure 3, the trajectory with a lot of sample number n can be optimized in a short time. The terminal condition in the iteration is given as

$$|\, J_s(i-k) - J_s(i-k-1)\,| < \xi,\ k = (0,1,2), \quad (42)$$

where,

$$J_s = J/n. \quad (43)$$

J is the cost function as shown in the equation (27). n is the sample number. Here, the relation between the evaluation value J_s and the sampling period Δt is shown in Figure 4. As seen from Figure 4, the evaluation J_s is converged with decreasing the sampling period Δt. Therefore, the trajectory is optimized quickly by giving the appropriate finish condition. In this study, we define the finish condition with $\xi = 0.1$, that is selected by the relation between the evaluation J_s and the sampling period Δt as shown in Figure 4.

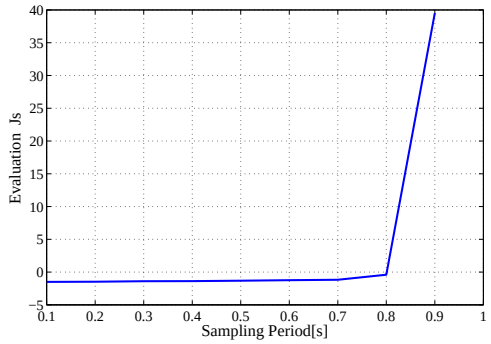

Figure 4: Relation between evaluation J_s and sampling period.

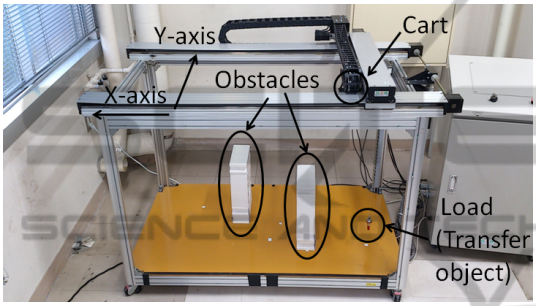

Figure 5: Overhead traveling crane system.

5 EXPERIMENTAL VALIDATION USING OVERHEAD TRAVELING CRANE

The effectiveness of the proposed method is validated by the experiments using laboratory overhead traveling crane as shown in Figure 5. The load as the transfer object is suspended to the cart by the rope. The travel range of the cart on X- and Y-axes are 1.2[m] and 0.5[m], respectively. And the maximum rope length is 0.85[m]. The cart traveled on X- and Y-axes is driven by a servomotor and a belt-and-pulley mechanism on each axis. The rope is reeled by a servomotor and a pulley. The cart position can be detected by rotary encoders attached to the servomotor on each axis. The rope length can also be detected by a rotary encoder attached the servomotor. The sway angle of the rope with the load can be detected by a laser range sensor system. The constraints to the cart transfer are shown in Table 1. The time constants and the gains of the motors represented as a first order delay system are shown in Table 2. The position feedback control systems are constructed to the motors on X- and Y-axes, respectively. The proportional control with the both gains, $K_p = 100$ are applied to the position feedback control systems.

Table 1: Constraints of transfer system.

	X-axis	Y-axis
Velocity[m/s]	± 0.35	± 0.35
Acceleration[m/s^2]	± 0.5	± 0.5
Input voltage[V]	± 10	± 10

Table 2: Parameters of motors.

	X-axis	Y-axis
Gain[m/s/V]	0.0361	0.0358
Time constant[s]	0.011	0.015

The experimental conditions to the laboratory overhead traveling crane system are shown as follows.

- Target position of the cart transfer is located as 1.0[m] and 0.4[m] on the X- and Y-axes, respectively.
- The range of the rope length while the cart transfer is between 0.3[m] and 0.7[m]. Therefore, the natural angular frequency of the load vibration is varied between 3.74[rad/s] and 5.72[rad/s]. The frequency band for suppressing the vibration is set to the range between 3.74[rad/s] and 5.72[rad/s] in the trajectory planning of the cart transfer on X- and Y-axes.
- Two obstacles covered into the ellipses are put into the transfer space. The size of the obstacles are same as 0.08[m] length of ellipse on X-axis and 0.25[m] length on Y-axis. The center positions of the ellipses are located on [0.35 0] and [0.75 0.4].
- The weight coefficients are given as $w_1 = 1$, $w_2 = 1$ and $w_3 = 1$ in case of the trajectory considering with the vibration suppression. For comparison, another experiment with the weight coeffieients $w_1 = 1$, $w_2 = 0$ and $w_3 = 0$, is performed. It is not considered with the vibration suppression.
- The transfer time is set to 6[s], and the sampling period on the transfer control is 0.01[s].

In the procedure of the fast solution as shown in Figure 3, the series of the sampling period for optimizing is given as $\Delta t = [1 \ 0.5 \ 0.25 \ 0.1]$. And in the terminal condition shown in the equation (42), the evaluation is selected as $k = 0$.

The experimental results of the cart transfer on X- and Y-axes are shown in Figures 6 and 7, respectively. In these figures, (a), (b), (c) and (d) show the cart positions, the velocities, the accelerations and the control inputs, respectively. In (b) and (c), the broken lines

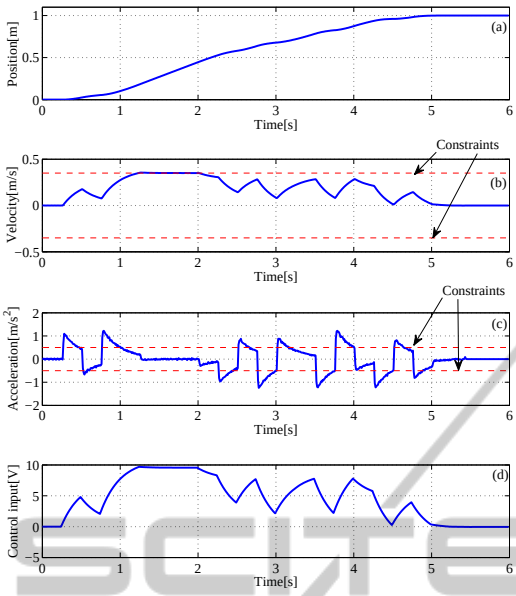

Figure 6: Experiment results on X-axis.

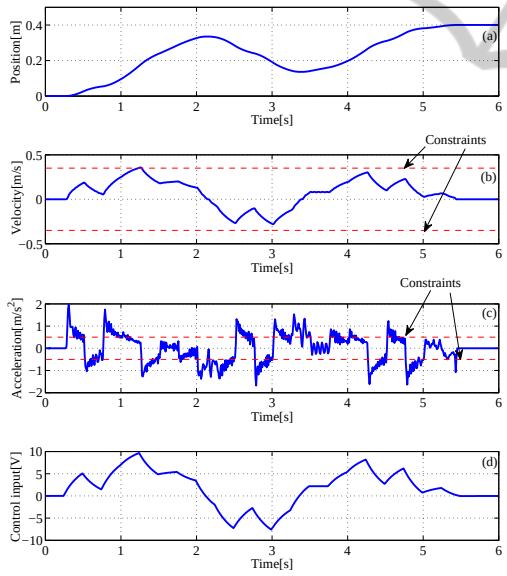

Figure 7: Experiment results on Y-axis.

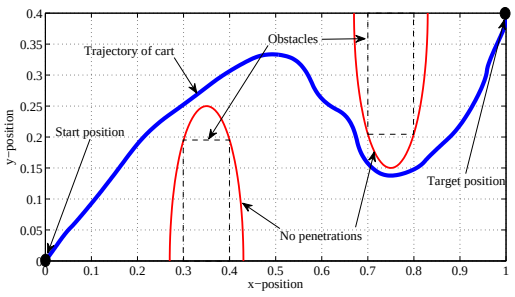

Figure 8: Experiment results in transfer trajectory.

Table 3: Calculation times.

	Computation time[s]
Conventional solution (Once optimization)	1484.00
Fast solution proposed in this study	5.85

are the constraints to each state. The control inputs are within the constraints. However, the velocities and the accelerations are exceeded. In this approach, since the sample period in the trajectory derived from the terminal condition in the fast solution is longer than that of the transfer control, the sample period of the trajectory is adjusted to that of the controller by the linear-interpolation method. By this procedure, the velocities and the accelerations can be exceeded. In order to solve this problem, interpolating smoothly the trajectory will be required in the future.

The trajectory on X- and Y-axes is shown in Figure 8. In Figre 8, the blue bold line is the trajectory of the transfer object, and the red thin lines are the no penetration areas. The black broken lines show the edges of the obstacles. As seen from Figure 8, the transfer object avoids the obstacles, and reachs the target position. The power spectrum of the input control is shown in Figure 9. The blue bold lines show the control input considering the vibration suppression, and the green thin lines show the that without the vibration suppression. In the power spectrum of the frequency bands 3.74[rad/s] to 5.72[rad/s], the spectrum with considering the vibration suppression is reduced. Therefore, the vibration considered in the proposed method can not be excited. The experimental results of the vibrations with the natural angular frequencies 3.74[rad/s] and 5.72[rad/s] are shown in Figures 10 and 11, respectively. The blue bold lines show the results by the proposed method considering vibration suppression, and the green thin lines show the results without vibration suppression. In Figures 10 and 11, it is seen that the vibration is suppressed by the proposed method. The calculation time compared between the fast solution proposed in this study and the conventional solution which the trajectory optimization is performed only once by the sample period 0.01[s], as shown in Table 3. The proposed optimization process is much faster than the conventional optimization process.

6 CONCLUSIONS

We proposed the trajectory planning method for 2-D load transfer machine including vibration element.

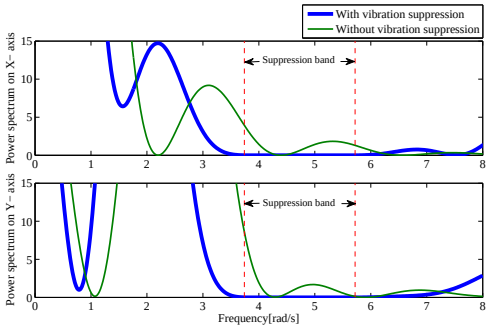

Figure 9: Power spectrums of control inputs.

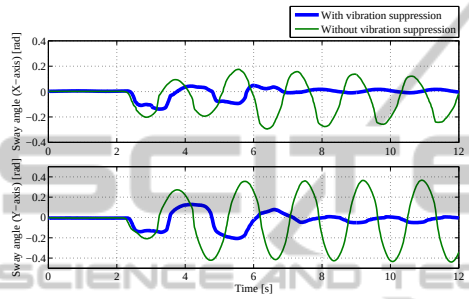

Figure 10: Experiment results of vibration with natural angular frequency 3.74[rad/s] (Rope length:0.7[m]).

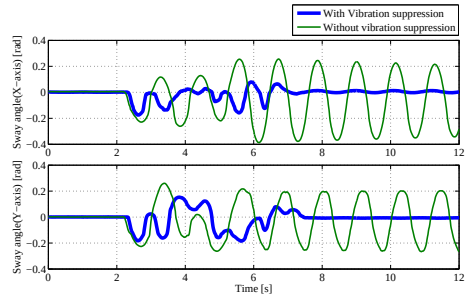

Figure 11: Experiment results of vibration with natural angular frequency 5.72[rad/s] (Rope length:0.3[m]).

The proposed method makes the transfer object avoid the obstacles, the motion suppress the vibration in the transfer object, and the state and the control input keep under the constraints. Moreover, the fast solution which shorten the calculation time of the trajectory optimization has been proposed in this study. In the experiments for validating the proposed method, it was seen that the vibration suppression, the obstacles avoidance are accomplished. In the future works, we will discuss the smooth interpolation method so that the velocity and the acceleration of the transfer object fall within the constraints.

REFERENCES

Kawakami, S, Miyoshi, T and Terashima, K, Path Planning of Transferred Load Considering Obstacle Avoidance for Overhead Crane, System Integration Division Annual Conference, p.640-641, 2003

Negishi, M, Masuda, H, Ohsumi, H and Tamura, Y, Evaluation of overhead crane trajectory, JSME Conference on Robotics and Mechatronics, p.1A2-p19(1)-(4), 2013

Yano, K, Eguchi, K and Terashima, K, Sensor-Less Sway Control of Rotary Crane Considering the Collision Avoidance to the Ground, Transactions of the Japan Society of Mechanical Engineers, Series(C), Vol. 68, No. 676, p.146-153

A. Z. Al-Garni, K. A. F. Moustafa and S. S. A. K. Javeed Nizami, Optimal Control of Overhead Cranes, Control Eng. Practice, Vol.3, No.9, p.1277-1284, 1995

Takagi, K, and Nishimura, H, Gain-Scheduled Control of A Tower Crane Considering Varying Load-Rope Length, Transactions of the Japan Society of Mechanical Engineers, Series(C), Vol. 64, No. 626, p.113-120

Harald, A and Dominik, S, Passivity-Based Trajectory Control of and Overhead Crane by Interconnection and Damping Assignment, Motion and Vibration Control , p.21-30, 2009

Murakami, S and Ikeda, T, Vibration suppression for High Speed Position Control of overhead Traveling Crane by Acceleration Inputs, Dynamics & Design Conference, p.128(1)-(6), 2006

Brunner, M, Bruggemann, B, and Schulz, D, Autonomously Traversing Obstacle: Metrics for Path Planning of Reconfigurable Robots on Rough Terrain, Proceedings of 9th International Conference on Informatics in Control, Automation and Robotics, p.58-69, 2012

Yu-Cheng, C, Wei-Han, H, Shin-Chung, K, A fast path planning method for single and dual crane erections, Automation in Construction, Volume 22, p. 468-480, 2012

Tamura, Y, Hamasaki, S, Yamashita, A and Asama, H, Collision Avoidance of Mobile Robot Based on Prediction of Human Movement According to Environments, Transactions of the Japan Society of Mechanical Engineers, Series(C), Vol. 79, No. 799, p.617-628

Suzuki, M and Terashima, K, Three Dimensional Path Planning using Potential Method for Overhead Crane, Journal of Robotics Society of Japan, Vol.18, No.5, p.728-736, 2000